UDC 621.314 https://doi.org/10.20998/2074-272X.2023.5.03

K. Djazia, M. Sarra

Improving the quality of energy using an active power filter with zero direct power command control related to a photovoltaic system connected to a network

Introduction. *This article's subject is a dual function energy system that improves the quality of the electric energy with help of an active power filter and uses a new technique of command named ZDPC (Zero Direct Power Command) on one hand, and on the other hand it injects the photovoltaic (PV) renewable energy to the electrical networks in the presence of non-linear charges. The* ***novelty*** *of the work consists in the subtraction of disturbances resulting from the non-linear charges is provided by an active power filter based on a new ZDPC method.* ***Methods.*** *This strategy combines a classic PI controller for DC bus voltage regulation with a smart method to maximum power point tracking (MPPT) of power based on fuzzy logic.* ***Purpose.*** *The elimination of the undesirable harmonics from the source currents makes the current almost sinusoidal with a harmonic distortion rate close to 1 %. The injection of PV energy into the electrical grid is provided by a PV panel in series with a chopper through a two-state inverter.* ***Results.*** *This system is simulated using MATLAB/Simulink software. The results prove the robustness and feasibility of the ZDPC control which simultaneously guarantees the compensation of harmonic currents, the correction of the power factor and the injection of the solar power into the electrical grid.* References 16, table 3, figures 20.

Key words: **active power filter, zero direct power command, photovoltaic array, fuzzy logic maximum power point tracking controller.**

Вступ. *Предметом цієї статті є енергосистема подвійного призначення, що покращує якість електроенергії за допомогою фільтра активної потужності та використовує, з одного боку, нову техніку управління під назвою ZDPC (Zero Direct Power Command), а з іншого боку, фотоелектричні відновлювані джерела енергії в електричні мережі за наявності нелінійних зарядів.* ***Новизна*** *роботи полягає в тому, що віднімання перешкод, що виникають від нелінійних зарядів, забезпечується фільтром активної потужності на основі нового методу ZDPC.* ***Методи***. *Ця стратегія поєднує класичний ПІ-регулятор для регулювання напруги на шині постійного струму з інтелектуальним методом відстеження точки максимальної потужності (MPPT) на основі нечіткої логіки.* ***Мета***. *Усунення небажаних гармонік із струмів джерела робить струм майже синусоїдальним з коефіцієнтом гармонічних спотворень, близьким до 1 %. Подача фотоелектричної енергії в електричну мережу забезпечується фотоелектричною панеллю, послідовно з'єднаної з переривником через інвертор з двома станами.* ***Результати***. *Ця система моделюється за допомогою програмного забезпечення MATLAB/Simulink. Результати доводять надійність та здійсненність управління ZDPC, яке одночасно гарантує компенсацію гармонічних струмів, корекцію коефіцієнта потужності та подачу сонячної енергії в електричну мережу.* Бібл. 16, табл. 3, рис. 20.

Ключові слова: **фільтр активної потужності, команда прямої нульової потужності, фотогальванічна батарея, контролер відстеження точки максимальної потужності з нечіткою логікою.**

Introduction. Harmonic pollution affects all domestic and industrial networks. No modern environment can escape this pollution from equipment, such as computers, servers, air conditioners, variable speed drives, etc... all these charges are called «non-linear». These equipments generate harmonic currents, which cause reactive power consumption and a degradation of the power factor of the electrical network [1, 2]. The quality of the current and the voltage of the network are seriously degraded [3-5].

The combination of a shunt active power filter (SAPF) and a photovoltaic (PV) source, which is not only a renewable source, but also clean, unlimited and at a very low level of risk; the purpose of the photovoltaic generator (GPV) is to inject the active power into the electrical grid. This combination gives us a clean source of energy and efficiently enhances the quality of energy [2, 6]. SAPF injects a current that opposes the harmonic current emitted by the non-linear charge to mitigate the effect of the harmonic currents and the reactive power. Thus, the current delivery by the power source remains sinusoidal.

Researchers have suggested new methods, such as direct power control (DPC) introduced by Noguchi [8], which was developed from direct torque control (DTC) intended for electric machine drives [3, 7].

DPC was essentially to remove both the pulse width modulation modulator and the internal regulation loops by through replacing them by a predetermined switching table [3]. This switching table, based on the correction of the active and reactive power and on the sector indicating the position angle of the source voltage vector, is intended to select the switching states of the converter [8].

The standard DPC requires a zero reactive power reference, whereas the active power reference is calculated from the DC bus controller output [3, 9]. This article proposes a DPC technique, which as opposed to the standard implementation, requires zero active and reactive power disturbance references to reject all disturbances due to harmonics. This is why we call it zero DPC or ZDPC (Zero Direct Power Command).

Given that the solar insulation is variable, several maximum power point tracking (MPPT) algorithms, such as incremental conductance, perturb and observe, and escalation have been proposed [2]. The tracking algorithm based on fuzzy logic, is considered to be on of the most efficient algorithms [10]. In our research the maximum power point (MMP) is reached smartly regardless of the degree of variation of the solar radiation due to the fuzzy MPPT technique [2].

Description of the studied model. The model studied in Fig. 1 consists of a solar GPV connected to the DC bus of a three-phase voltage inverter through a chopper circuit, coupled in parallel to the network through an inductance. This electrical network supplies a non-linear receiver constituted by a rectifier PD3 whose charge is a resistor in series with an inductance. The synoptic of Fig. 1 illustrates this configuration with ideal flow of powers. The analysis of these flows is therefore

examined in various regimes imposed by the fluctuation of the level of irradiation during the day and the alternation with the night part where only the functions of the active filter are activated. During the day, depending on the levels of irradiation and the consumption of the charge, it is possible to distinguish several regimes (P_{pv} is the PV active power; P_{charge} is the load active power):

- $P_{pv} < P_{charge}$, the network power remains positive;
- $P_{pv} > P_{charge}$, the network receives an active power, it becomes a receiver.

These power flow management phases are coupled with the active filter functionalities. The voltage inverter control algorithm is adapted to simultaneously ensure the compensation of the harmonic pollution and of the reactive power, and also the injection of the power supplied by the PV panels into the electrical network.

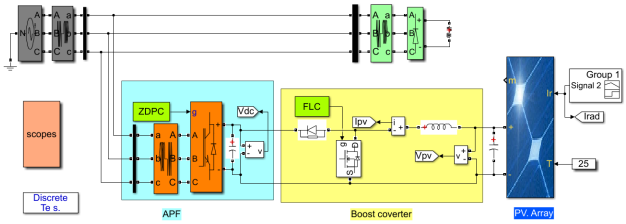

Fig. 1. Synoptic studied model

The proposed ZDPC principle. Figure 2 shows the structure of the proposed ZDPC. In this control strategy, the active and reactive power disturbance references are set to zero. We note that in this structure the phase locked loop is not necessary [3]. The high selective filter (HSF) is used to separate the fundamental and harmonic components of the line currents and voltages in order to perform power compensation [3].

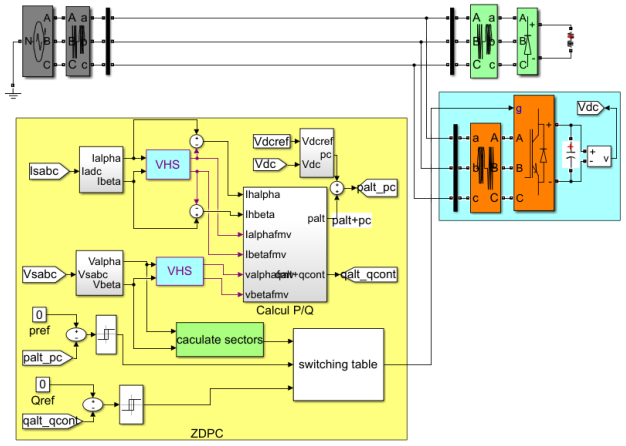

Fig. 2. Synoptic of the ZDPC

Choice of sector. The signal d_{ps}, d_{pq} and the position (θ) of the source voltage vector (1), from a digital word, allowing access to the address of the switch table to select the appropriate voltage vector:

$$\theta = \text{arctg}\left(v_\alpha / v_\beta\right). \qquad (1)$$

For this reason, the stationary coordinates are divided into 12 sectors (Fig. 3), and the sectors can be expressed numerically as [3]:

$$(n-2).\frac{\pi}{6} \le \theta_n \le (n-1).\frac{\pi}{6} \quad n = 1,2,....,12\,. \qquad (2)$$

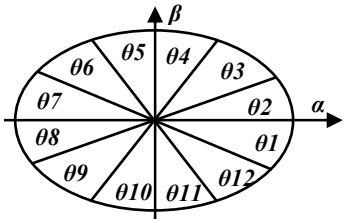

Fig. 3. (α, β) sectors

The signals d_{ps}, d_{qs} and the sector n of the source voltage are the inputs of the commutation table (Table 1), whereas the output represents the switching state of the inverter (S_a, S_b, S_c). By using this switching table, the optimal state of the inverter can be uniquely selected during each time interval depending on the combination of the table entries. The selection of the optimal switching state is made so that power errors can be reduced in the hysteresis bands.

Table 1

ZDPC switching table

d_p	d_q	θ_1	θ_2	θ_3	θ_4	θ_5	θ_6	θ_7	θ_8	θ_9	θ_{10}	θ_{11}	θ_{12}
1	0	v_6	v_7	v_1	v_0	v_2	v_7	v_3	v_0	v_4	v_7	v_5	v_0
	1	v_7	v_7	v_0	v_0	v_7	v_7	v_0	v_0	v_7	v_7	v_0	v_0
0	0	v_6	v_1	v_1	v_2	v_2	v_3	v_3	v_4	v_4	v_5	v_5	v_6
	1	v_1	v_2	v_2	v_3	v_3	v_4	v_4	v_5	v_5	v_6	v_6	v_1
$v_1(100)$, $v_2(110)$, $v_3(010)$, $v_4(011)$, $v_5(001)$, $v_6(101)$, $v_0(000)$, $v_7(111)$													

Hysteresis controller. The main idea of the ZDPC method is to keep the instantaneous active and reactive power within a desired band. This command is based on two comparators with hysteresis whose input is the error between the reference values and the estimate of the active and reactive power [11], given respectively as:

$$\Delta p_s = p_{ref} - p_s\,; \qquad (3)$$

$$\Delta q_s = q_{ref} - q_s\,. \qquad (4)$$

where p_{ref}, q_{ref} are the instantaneous active and reactive power reference; p_s, q_s are the instantaneous active and reactive power source.

The hysteresis comparators are used to provide 2 logic outputs d_{ps} and d_{qs}. State «1» corresponds to an increase in the controlled variable (ps and qs), whereas «0» corresponds to a decrease according to (5), (6)

$$\text{if } \Delta p_s \ge h_p \;\; d_{ps} = 1;\ \text{if } \Delta p_s \le -h_p \;\; d_{ps} = 0\,; \qquad (5)$$

$$\text{if } \Delta q_s \ge h_q \;\; d_{qs} = 1;\ \text{if } \Delta q_s \le -h_q \;\; d_{qs} = 0\,. \qquad (6)$$

PI controller. The ZDPC method must ensure DC bus regulation to maintain the capacitor voltage, around the voltage reference (V_{dcref}). For this purpose, a PI controller is usually used [11]. Figure 4 shows the controller simulation model.

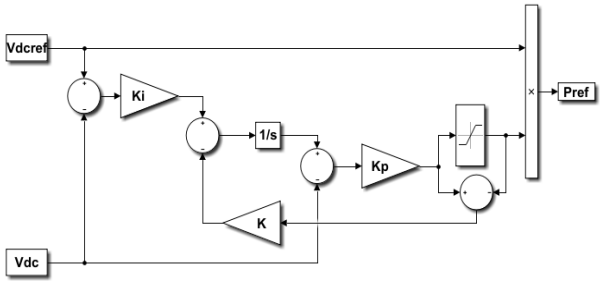

Fig. 4. Simulation model of PI controller

The values of proportional and integral gain (K_p and K_i) are given respectively as:

$$K_i = \frac{\omega_n}{2\zeta}; \tag{7}$$

$$K_p = 2C\zeta\omega_n, \tag{8}$$

where ξ is the damping coefficient (ξ = 0.707); ω_n is the nominal pulse.

High selective filter. To improve the performance of the classical instantaneous power method, HSF has been implemented, to extract the fundamental component of current and voltage in the synchronous frame without any phase shift or amplitude errors. The functional diagram of HSF is shown in Fig. 5. The transfer function can be expressed as [11]:

$$H(s) = \frac{\hat{x}_{\alpha\beta}(s)}{x_{\alpha\beta}} = k\frac{(s+k)+j\omega_c}{(s+k)^2+\omega_c^2}. \tag{9}$$

From (9), we obtain:

$$\hat{x}_\alpha(s) = \frac{k}{s}\left[x_\alpha(s) - \hat{x}_\alpha(s)\right] - \frac{\omega_c}{s}\hat{x}_\beta(s); \tag{10}$$

$$\hat{x}_\beta(s) = \frac{k}{s}\left[x_\beta(s) - \hat{x}_\beta(s)\right] - \frac{\omega_c}{s}\hat{x}_\alpha(s), \tag{11}$$

where $\hat{x}_{\beta\alpha}$, $x_{\alpha\beta}$ are respectively the output and the input of the filter, which can be $V_{\alpha\beta}$ or $I_{\alpha\beta}$. We note that for the pulsation $\omega = \omega_c$, the phase shift introduced by the filter is zero and the gain is equal to 1. We also observe that the decrease in the value K improves the selectivity of the HSF.

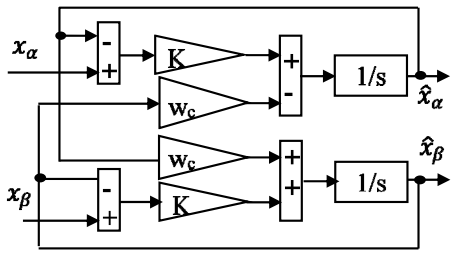

Fig. 5. Block diagram of HSF

From the HSF output, the AC component of the instantaneous active power can be obtained by (12) [3]:

$$\tilde{p} = \hat{v}_\alpha i_{h\alpha} + \hat{v}_\beta i_{h\beta}, \tag{12}$$

where $i_{h\alpha}$, $i_{h\beta}$ given respectively by (13) and (14):

$$i_{h\alpha} = \left(i_{\alpha d} - \hat{i}_{\alpha d}\right) + \left(i_{\alpha inv} - \hat{i}_{\alpha inv}\right); \tag{13}$$

$$i_{h\beta} = \left(i_{\beta d} - \hat{i}_{\beta d}\right) + \left(i_{\beta inv} - \hat{i}_{\beta inv}\right), \tag{14}$$

where $i_{h\alpha}$, $i_{h\beta}$ are the harmonic components in the axis $\alpha\beta$, whereas the instantaneous reactive power is defined as:

$$q_s = \hat{v}_\beta \hat{i}_\alpha - \hat{v}_\alpha \hat{i}_\beta. \tag{15}$$

Figure 6 shows the calculation of the disturbing powers $\tilde{p}$ and q_s.

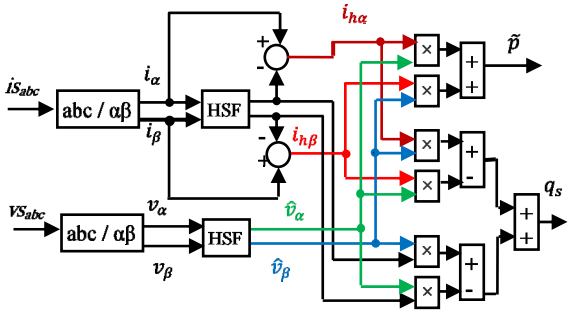

Fig. 6. Computation of v_α, v_β, $\tilde{p}$ and q_s with HSF

Generation of control vector. By adding the alternating component ($\tilde{p}$) of the instantaneous active power which is linked to both current and voltage disturbances, to the active power p_c necessary for the regulation of the DC bus, we obtain the disturbing active power p_p:

$$p_p = \tilde{p} + p_c. \tag{16}$$

To compensate for active and reactive power disturbances (p_p and q_s), a comparison with their zero reference is carried out. The results of the comparison pass through a hysteresis block which generates output hysteresis controller (dps and dqs). Depending on the sector selected (θ_n) and (d_{ps}, d_{qs}), the appropriate command vector (S_a, S_b, S_c) is produced using the commutation table (Table 1).

Advanced MPPT controller. The extraction of the maximum power is an essential step in the field of energy conversion of the PV solar system. To increase the efficiency of the GPV, a MPPT search algorithm is applied to the DC/DC converter (local MPPT) in the case of a double power stage. In this article the algorithm based on fuzzy logic is studied. This method is used here for finding the MPPT of a PV module under all weather conditions, because it does not require knowledge of mathematical models of linear and nonlinear controlled systems [12, 13].

Generally, the fuzzy logic controller comprises 3 essential blocks: fuzzification, inference rules and defuzzification [14]. The fuzzification stage is the process of transforming numerical input variables into linguistic variables using membership functions. The inference rules step gives the output of the fuzzy logic controller by the Mamdani method with a max-min technique depending on the set belonging to the rule base. The defuzzification step converts the linguistic variables into a net value, which determines the duty cycle increment ΔD. The fuzzy MPPT values are represented by an E error and an ΔE error variation as inputs. The error and its variation are given by the following equations [13]:

$$E(K) = \frac{P(K) - P(K-1)}{V(K) - V(K-1)}; \tag{17}$$

$$\Delta E = E(K) - E(K-1), \tag{18}$$

where $P(k)$, $P(k–1)$, $V(k)$ and $V(k–1)$ are the power and the voltage of the GPV for 2 sampling times k and (k–1) respectively. The proposed algorithm has 2 input variables: $\Delta P(k)$ and $\Delta V(k)$. The output variable is the duty cycle $\Delta D(k)$. The variables $\Delta P(k)$ and $\Delta V(k)$ are given as [13, 14]:

$$\Delta P(K) = P(K) - P(K-1); \tag{19}$$

$$\Delta V(K) = V(K) - V(K-1). \tag{20}$$

where $\Delta P(k)$ and $\Delta V(k)$ are zero at the MPP of the GPV.

The basic rules of the fuzzy MPPT algorithm are based on the 2 input variables ($\Delta P(k)$, $\Delta V(k)$) and on the output variable (ΔD). $\Delta P(k)$ and $\Delta V(k)$ are divided into 5 denoted fuzzy sets: Negative Big (*NB*), Negative Small (*NS*), Zero (*Z*), Positive Small (*PS*) and Positive Big (*PB*). The rule base relates the fuzzy inputs to the fuzzy output by the master syntax rule: «If: *A* is... and *B* is..., Then: *C* is...». According to Table 2 [13, 14], that groups together

all the possible connections between the inputs and the output of the developed controller, the following example can be given: If: ΔP is *PB* and ΔV is *NB* Then: ΔD is *NS*. The choice of the shape of the membership functions of the proposed controller is of a triangular type. The center of gravity method for the defuzzification step is used to calculate the incremental duty cycle ΔD [10, 14-16]:

$$\Delta D = \frac{\sum_{j=0}^{n} \omega_j \Delta D_j}{\sum_{j=0}^{n} \omega_j}, \qquad (21)$$

where n is the maximum number of effective rules, w is the weighting factor, ΔD_j is the value corresponding to ΔD.

Table 2

Decision table

$\Delta P \backslash \Delta V$	NB	NS	Z	PS	PB
NB	PS	PB	PB	NB	NS
NS	Z	PS	PS	NS	Z
Z	Z	Z	Z	Z	Z
PS	Z	NS	NS	PS	Z
PB	NS	NB	NB	PB	PS

Finally, the duty cycle is obtained by adding this change to the previous value of the control duty cycle as mentioned in (22) [10, 14, 15]:

$$D(K+1) = D(K) + \Delta D(K). \qquad (22)$$

Discussion of the simulation results. Various simulations were performed using MATLAB/Simulink model (Fig. 1) to evaluate the proposed approaches. The parameters used for these tests are represented in Table 3.

Table 3

Simulation parameters

Parameters	Value	Parameters	Value
V_s, V	80	C_{dc}, µF	2200
f_s, Hz	50	L, mH	10
f switching (DC/AC APF converter), kHz	20	R, Ω	40
f switching (DC/DC boost converter), kHz	5	C_{pv}, µF	20
L_s, mH	0.1	L_{pv}, mH	3
R_s, Ω	0.1	V_{cref}, V	235
L_l, mH	0.566	N	2
R_l, Ω	0.01	ω_b, rad/s	0,01
L_f, mH	2.5	ω_h, rad/s	100
R_f, Ω	0.01		

SAPF simulation results controlled by the ZDPC, equipped with conventional PI and fuzzy MPPT, operating under a balanced network, are shown in the following figures. Figure 7 shows all simulated cases together during time (0 – 1.4) s. Figure 8 zooms the signals in the time interval (0 – 0.2) s, where the filter is not activated and in the absence of irradiation (absence of the injection of energy to the network), in this case we notice the load current and the source current are identical as shown in Fig. 9.

The charge current and the source current are superimposed and have a total harmonic distortion (THD) 27.87 % (Fig. 10).

Figure 11 shows the signals after the activation of the APF and in the absence of irradiation during the time interval (0.2-0.5) s.

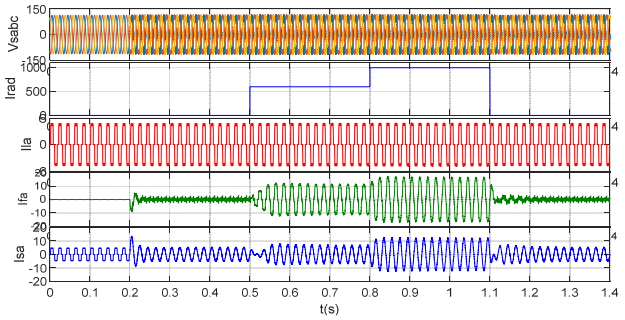

Fig. 7. Simulation signals in the different cases

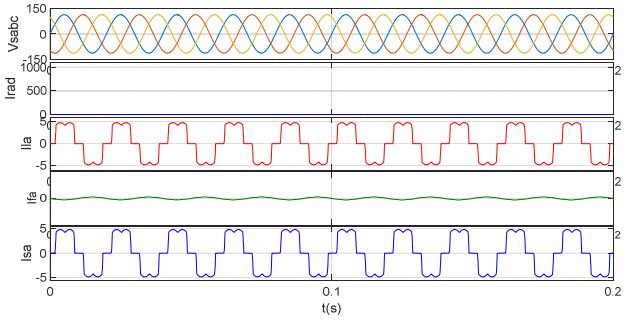

Fig. 8. Simulation signals in the absence of the filter and of irradiation

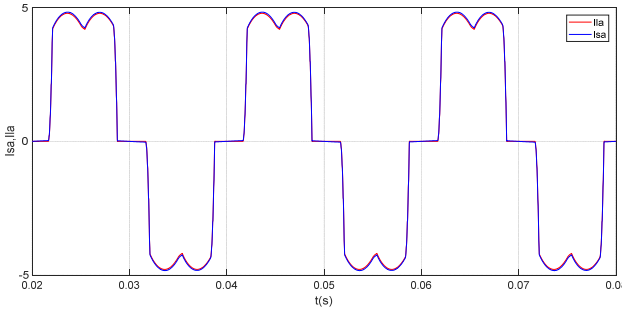

Fig. 9. The charge current and the source current are superimposed

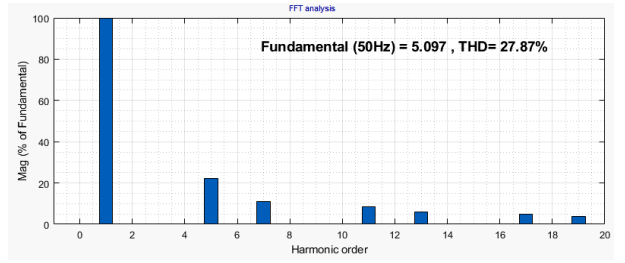

Fig. 10. THD of source current

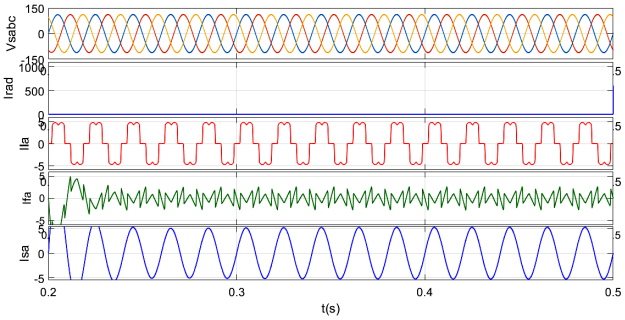

Fig. 11. Simulation signals after the activation of the APF and in absence of irradiation

It is noted in Fig. 12 that the source current resumes its sinusoidal form in phase with the charge current and with a THD = 1.14 % as shown in Fig. 13.

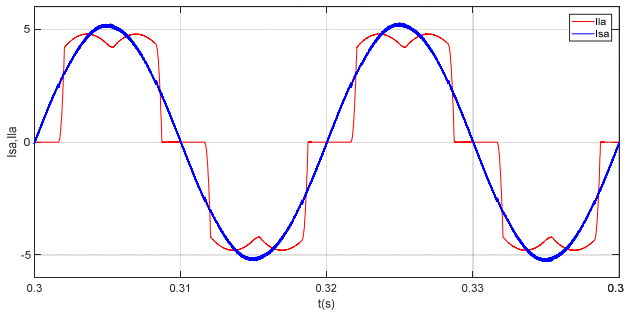

Fig. 12. The source current is in phase with the charge current

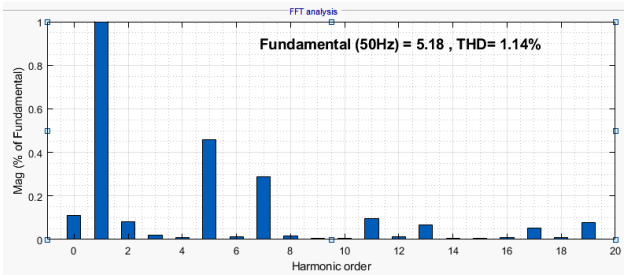

Fig. 13. THD of source current

Figure 14 represents the simulation signals during the activation of the APF and the injection of energy to the network, this is in the time interval (0.5-0.8) s, in this case the source current changes direction towards the network and becomes in phase opposition with the charge current, which means that the network becomes a receiver. The source current has a THD = 1.09 %

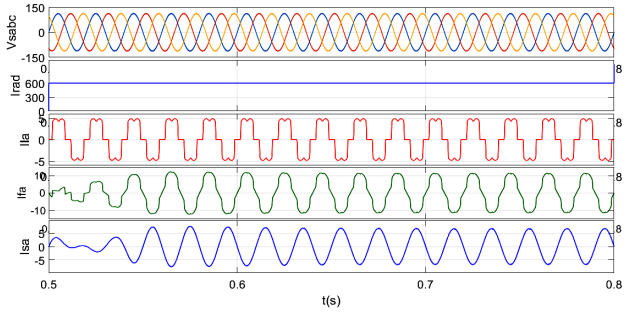

Fig. 14. Simulation signals after the activation of the APF and with the presence of irradiation

Figure 15 shows the transition from the network to a receiver. The source current retains its sinusoidal shape with a THD = 1.09 % (Fig. 16).

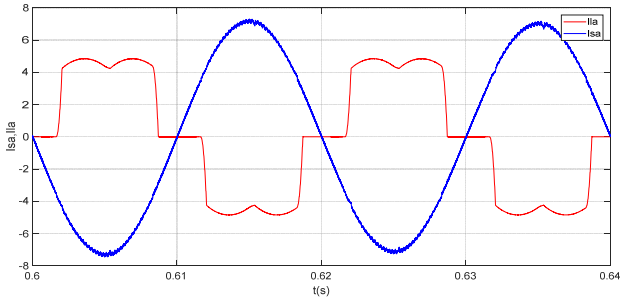

Fig. 15. The source current is in phase opposition with the charge current

Figures 17, 18 show the crossing of the source current with that of the irradiation while keeping the sinusoidal form of the source current with a THD = 1.29 % (Fig. 19).

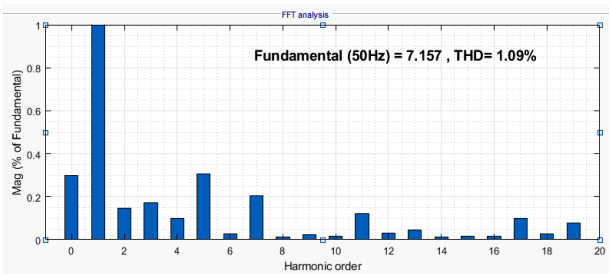

Fig. 16. THD of source current

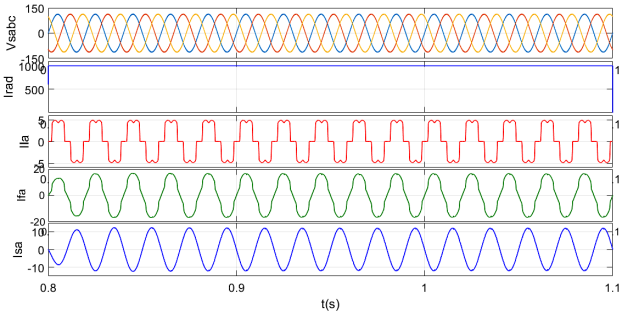

Fig. 17. Simulation during the increase in irradiation

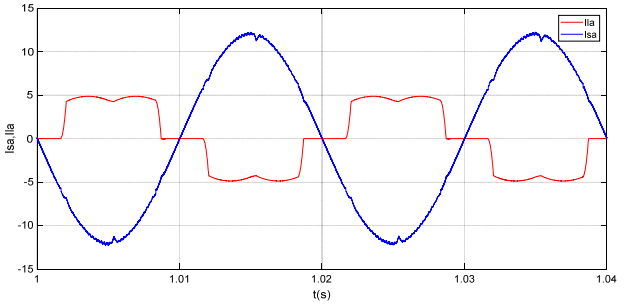

Fig. 18. Crossing of the source current with the irradiation current

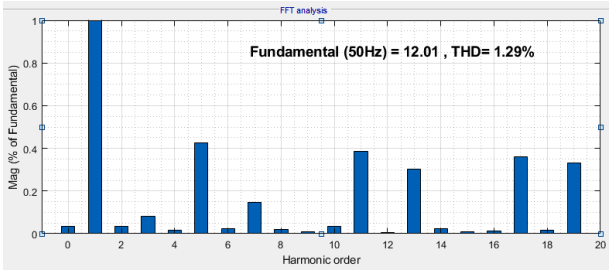

Fig. 19. THD of source current

Figure 20 shows the evolution of the energy of the network in the various cases discussed:

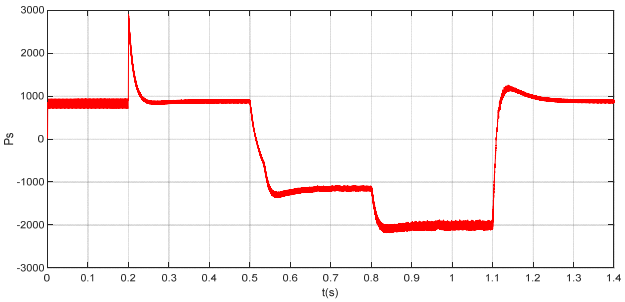

Fig. 20. Energy of the network in the different discussed cases

- Case 1: before activation of the APF and in the absence of irradiation.

- Case 2: after activation of the APF and in the absence of irradiation.
- Case 3: after the activation of the APF and in the presence of the irradiation.
- Case 4: during the change of irradiation.

Conclusions. In this article, a new direct power control technique called zero direct power control, suitable for harmonic and reactive power compensation, has been proposed; high selectivity filters are used to separate harmonic currents and voltages causing a degradation in the quality of power on the network. The shunt active power filter based on the zero direct power control command assembled with a photovoltaic system driven by a fuzzy command to inject energy into the network and improve the quality of energy. The simulation shows the good performance of the proposed approach.

Conflict of interest. The authors declare that they have no conflicts of interest.

REFERENCES

1. Mohamed Rida B., Rahli M., Slami S., Hassaine L. PSO based Direct Power Control for a Multifunctional Grid Connected Photovoltaic System. *International Journal of Power Electronics and Drive Systems (IJPEDS)*, 2018, vol. 9, no. 2, pp. 610-621. doi: https://doi.org/10.11591/ijpeds.v9.i2.pp610-621.

2. Boudechiche G., Sarra M., Aissa O., Gaubert J.-P. An investigation of solar active power filter based on direct power control for voltage quality and energy transfer in grid-tied photovoltaic system under unbalanced and distorted conditions. *Journal of Engineering Research*, 2021, vol. 9, no. 3B, pp. 168-188. doi: https://doi.org/10.36909/jer.v9i3B.9061.

3. Djazia K., Krim F., Chaoui A., Sarra M. Active Power Filtering Using the ZDPC Method under Unbalanced and Distorted Grid Voltage Conditions. *Energies*, 2015, vol. 8, no. 3, pp. 1584-1605. doi: https://doi.org/10.3390/en8031584.

4. Baazouzi K., Bensalah A.D., Drid S., Chrifi-Alaoui L. Passivity voltage based control of the boost power converter used in photovoltaic system. *Electrical Engineering & Electromechanics*, 2022, no. 2, pp. 11-17. doi: https://doi.org/10.20998/2074-272X.2022.2.02.

5. Sai Thrinath B.V., Prabhu S., Meghya Nayak B. Power quality improvement by using photovoltaic based shunt active harmonic filter with Z-source inverter converter. *Electrical Engineering & Electromechanics*, 2022, no. 6, pp. 35-41. doi: https://doi.org/10.20998/2074-272X.2022.6.06.

6. Tareen W.U., Mekhilef S., Seyedmahmoudian M., Horan B. Active power filter (APF) for mitigation of power quality issues in grid integration of wind and photovoltaic energy conversion system. *Renewable and Sustainable Energy Reviews*, 2017, vol. 70, pp. 635-655. doi: https://doi.org/10.1016/j.rser.2016.11.091.

7. Aissa O., Moulahoum S., Colak I., Kabache N., Babes B. Improved Performance and Power Quality of Direct Torque Control of Asynchronous Motor by Using Intelligent Controllers. *Electric Power Components and Systems*, 2016, vol. 44, no. 4, pp. 343-358. doi: https://doi.org/10.1080/15325008.2015.1117541.

8. Noguchi T., Tomiki H., Kondo S., Takahashi I. Direct power control of PWM converter without power-source voltage sensors. *IEEE Transactions on Industry Applications*, 1998, vol. 34, no. 3, pp. 473-479. doi: https://doi.org/10.1109/28.673716.

9. Mesbahi N., Ouari A., Ould Abdeslam D., Djamah T., Omeiri A. Direct power control of shunt active filter using high selectivity filter (HSF) under distorted or unbalanced conditions. *Electric Power Systems Research*, 2014, vol. 108, pp. 113-123. doi: https://doi.org/10.1016/j.epsr.2013.11.006.

10. Benlahbib B., Bouarroudj N., Mekhilef S., Abdelkrim T., Lakhdari A., Bouchafaa F. A Fuzzy Logic Controller Based on Maximum Power Point Tracking Algorithm for Partially Shaded PV Array-Experimental Validation. *Elektronika Ir Elektrotechnika*, 2018, vol. 24, no. 4, pp. 38-44. doi: https://doi.org/10.5755/j01.eie.24.4.21476.

11. Sujith M., Padma S. Optimization of harmonics with active power filter based on ADALINE neural network. *Microprocessors and Microsystems*, 2020, vol. 73, art. no. 102976. doi: https://doi.org/10.1016/j.micpro.2019.102976.

12. Chavan U.M., Thorat A.R., Bhosale S.S. Shunt Active Filter for Harmonic Compensation Using Fuzzy Logic Technique. *2018 International Conference on Current Trends towards Converging Technologies (ICCTCT)*, 2018, pp. 1-6. doi: https://doi.org/10.1109/ICCTCT.2018.8550962.

13. Boukezata B., Chaoui A., Gaubert J.-P., Hachemi M. An improved fuzzy logic control MPPT based P&O method to solve fast irradiation change problem. *Journal of Renewable and Sustainable Energy*, 2016, vol. 8, no. 4, art. no. 043505. doi: https://doi.org/10.1063/1.4960409.

14. Manoharan P., Subramaniam U., Babu T.S., Padmanaban S., Holm-Nielsen J.B., Mitolo M., Ravichandran S. Improved Perturb and Observation Maximum Power Point Tracking Technique for Solar Photovoltaic Power Generation Systems. *IEEE Systems Journal*, 2021, vol. 15, no. 2, pp. 3024-3035. doi: https://doi.org/10.1109/JSYST.2020.3003255.

15. Kumar A., Kumar P. Power Quality Improvement for Grid-connected PV System Based on Distribution Static Compensator with Fuzzy Logic Controller and UVT/ADALINE-based Least Mean Square Controller. *Journal of Modern Power Systems and Clean Energy*, 2021, vol. 9, no. 6, pp. 1289-1299. doi: https://doi.org/10.35833/MPCE.2021.000285.

16. Verma N., Jain A., Nishi, Ahuja H., Singh G. Maximum Power Point Tracking MPPT Methods for Photovoltaic Modules. *2021 International Conference on Advance Computing and Innovative Technologies in Engineering (ICACITE)*, 2021, pp. 223-227. doi: https://doi.org/10.1109/ICACITE51222.2021.9404571.

Received 17.12.2022
Accepted 10.02.2023
Published 01.09.2023

Kamel Djazia[1], *Doctor of Electronics,*
Mustapha Sarra[2], *Doctor of Electronics, Professor,*
[1] Department of Electronics, University of Msila, Algeria,
e-mail: kamel.djazia@univ-msila.dz (Corresponding Author);
[2] Department of Electronics,
University of Bordj Bou Arreridj, Algeria,
e-mail: mustapha.sarra@univ-bba.dz

How to cite this article:
Djazia K., Sarra M. Improving the quality of energy using an active power filter with zero direct power command control related to a photovoltaic system connected to a network. *Electrical Engineering & Electromechanics*, 2023, no. 5, pp. 20-25. doi: https://doi.org/10.20998/2074-272X.2023.5.03